

# Mechanisms of uniform corrosion under corrosion deposits

J. L. CROLET

*Elf-Aquitaine, 64018 Pau Cedex, France*

The liquid-phase transport phenomena which occur at the surface of iron-base alloys during corrosion have been analysed. These mechanisms determine either the maintenance of bare metal or the precipitation of solid corrosion products, the build-up of a corrosion deposit and the control of its thickness, and finally, the kinetics of the electrochemical reactions under the deposit. Although it is shown that pure "precipitation–redissolution" or "direct formation" reactions are impossible, the only conceivable mechanisms are nevertheless closely related, because the transport of iron between the metal and the external corrosive medium occurs chiefly either via the solid phase of the deposit (for "soluble" deposits), or via the liquid phase permeating its porosities (for "insoluble" deposits). It is also shown that, depending on the precipitation conditions, any given solid compound  $Fe_nX_2$  can lead to three types of deposit with quite different properties. (i) "Soluble" deposits: moderately protective, steady-state corrosion insensitive to potential, but highly sensitive to turbulence; (ii) "Insoluble cationic" deposits (controlled by the removal of  $Fe^{2+}$  cations by liquid-phase diffusion): highly protective, corrosion rate slightly sensitive to potential, and insensitive to turbulence. (iii) "Insoluble anionic" deposits (controlled by the diffusional supply of the precipitable anion  $X^{n-}$ ): slightly or unprotective, corrosion slight or insensitive to the presence of the deposit; possibly profuse deposit if steady state corrosion is not attained. This theoretical analysis can retrospectively explain numerous experimental observations reported in the literature, such as the incubation time before the drop in corrosion rates, the multiple forms of  $CO_2$  and  $H_2S$  corrosion, the role of  $Ca^{2+}$  ions, erosion–corrosion and bacterial corrosion. This analysis also paves the way for the reliable laboratory prediction of real corrosion rates under deposits.

## 1. Introduction

### 1.1. Origin of corrosion deposits and traditional mechanisms

The precipitation of corrosion products at the surface of a corroding metal is, by definition, a problem of solubility equilibrium; the real question is to know which equilibria are concerned.

In principle, it is clear that it is not an overall mean solubility of the corrosion products in the corrosive medium which is involved. In effect, under working conditions in an industrial installation, the volume available for dispersal of the corrosion products is practically infinite, so that their solubility limits could never be attained throughout the whole of the medium.

However, corrosion deposits are commonly observed, even in circulating corrosive media practically devoid of corrosion products [1]. Similarly, in laboratory tests, corrosion deposits are frequently found on specimens, even though their mean level of saturation in the test medium remains very low, and no deposits are effectively observed elsewhere. Thus, it is already apparent that the formation and growth of corrosion deposits can only be due to the presence or ab-

sence of local equilibria, dependent on kinetic phenomena.

The choice then remains between the kinetics of precipitation–redissolution reactions and those of liquid-phase transport. Here again, it is obvious that only a relative insufficiency of the transport kinetics can explain local enrichments, leading to precipitation of corrosion products in a medium whose mean level of saturation is almost zero everywhere else. On the contrary, the stability of the deposit and the steady state transport rate through it can depend equally on either factor [1].

1. In the case of the so-called "precipitation–redissolution" mechanism, it is assumed that the deposit forms continuously on the metal surface, and that it redissolves at the same rate at its outer interface. Between the metal and the external corrosive medium, all of the corroded iron therefore transits via the solid deposit.

2. In the case of the "direct formation" mechanism, it is assumed on the contrary that the deposit forms during an initial transient phase, but that thereafter, the solid produced no longer contributes to the kinetics of corrosion product removal.

## 1.2. Properties of corrosion deposits

In real situations, it is known from experience that, in many cases, the rate of corrosion of non-passivating metals is controlled by the more or less protective nature of the corrosion products [2-4]. Moreover, it is often quite difficult to reproduce these complex surface conditions, so that laboratory simulations and measurements are rarely representative of real behaviour. It is again evident that the more or less protective nature of the deposit must necessarily depend on the controlling mechanism involved. While the two mechanisms mentioned are often invoked in the literature, they have apparently never been analysed in detail.

The aim of the present study was therefore, to establish models for diffusion behaviour in this limiting surface layer of the corrosive medium, in an attempt to describe the exchange of matter and the various phenomena which can occur in the vicinity of the metal-solution interface. In this way, it was hoped to attain a better understanding of the formation, stability and protective effects of corrosion deposits.

It will be seen in particular that the two mechanisms mentioned, direct formation and precipitation-redissolution, cannot exist in a pure form, and that only hybrid phenomena can be envisaged in real situations, even if they conserve a marked resemblance to their pure equivalents. It will also be seen that there are three basic hybrid mechanisms, together with a continuum of intermediate ones. However, in spite of this continuity, the three basic hybrids each have highly specific characteristics, which make them clearly distinguishable from one another. In particular, their respective dependencies on electrochemical and hydrodynamic factors are profoundly different. This is also true for the tendency to show unstable uniform corrosion, which determines the possibility of developing local attack, especially in the case of corrosion by acid gases, or whenever the corrosion deposit is the salt of a weak acid.

Throughout all of this, it should not, of course, be forgotten that the underlying phenomenon is the corrosion of the bare metal.

## 2. Corrosion of bare metal

### 2.1. Potential corrosivity and real corrosivity

The chemical species involved in corrosion are electrons, and ions in solution [1]. They are therefore highly mobile. When a bare metal is immersed in a corrosive aqueous medium, the state of the interface, the metal-solution potential and the dynamic equilibrium between the anode and cathode reactions are set up in a few fractions of a second at the most. This almost immediate quasi-stationary state then slowly changes and eventually reaches a steady regime, after a time which can be highly variable, except in cases where, on the contrary, the corrosion rate shows a sudden sharp drop, due to the formation and growth of corrosion deposits.

The corrosion rate observed for the initial state of the interface corresponds to the "potential corrosivity" of the medium [2], i.e. to the dynamic equilibrium

between the anodic and cathodic reactions on a surface which has not yet been modified by the reaction products. On the contrary, the real corrosivity corresponds to the final corrosion rate when the stable steady-state interface has been established.

The potential corrosivity is therefore the initial corrosion rate of the bare metal, while the real corrosivity is often that of the metal covered by "real" corrosion deposits. Unfortunately, experience shows that the deposits obtained in the laboratory are frequently not the same as those observed in real situations [3, 5].

Until now, fundamental studies on electrochemical kinetics or corrosion mechanisms have dealt chiefly with bare or passivated metals [6], or with established deposits, and have rarely considered their formation and growth. However, it is the latter stage which determines the future properties of the deposit, and which therefore defines the conditions which must be respected for any laboratory simulation. Similarly, because of the difficulty in obtaining representative measurements of the real corrosivity, for the technological evaluation of corrosion risks, it is often preferred, for safety reasons, to use the potential corrosivity [4]. Such an approach can lead to excessive precautions, which can become extremely costly in industries where the technical and economic stakes are high.

For all these reasons, therefore, it is important to determine why a corroding metal remains bare or why it becomes covered with a corrosion deposit. In short, what is the modification at the metal-solution interface which brings about this change?

### 2.2. Dispersal of corrosion products

#### 2.2.1. Diffusion in the liquid phase

A steel which dissolves at a uniform rate of  $v$  (mm/yr) injects a constant flux of iron,  $J$ , at the liquid surface (Fig. 1). The correspondence between "corrosion" units and "diffusion" units gives

$$|J|(\text{mg cm}^{-2} \text{s}^{-1}) = 2.5 \times 10^{-5} v(\text{mm/yr}) \quad (1a)$$

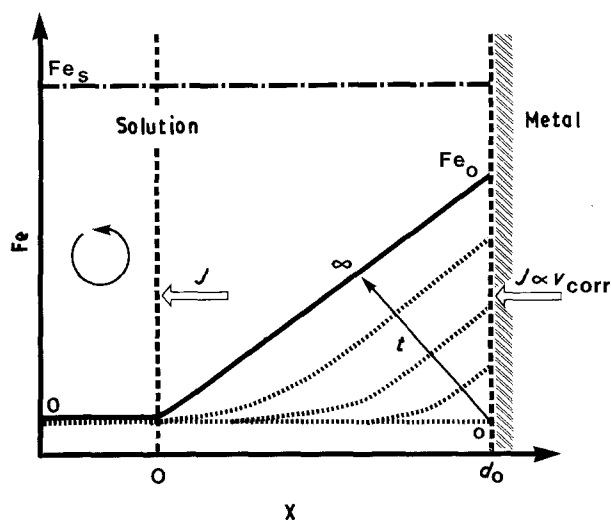


Figure 1 Build-up of an iron concentration gradient perpendicular to the surface of a corroding bare metal.

Later on, it will be necessary to express this flux, not in diffusion units, such as  $\text{mg cm}^{-2} \text{s}^{-1}$ , but in terms of the concentration unit usually employed in corrosion electrochemistry, i.e. in  $\text{meq l}^{-1}$

$$|J|(\text{meq l}^{-1})(\text{cm s}^{-1}) = 10^{-3} v(\text{mm/yr}) \quad (1b)$$

In the stationary state, this flux  $J$  is dispersed continually throughout the volume of the corrosive medium. Once it has reached the convective zone of the liquid, the dispersal occurs easily. However, it must first penetrate through the boundary diffusion layer, of thickness  $d_0$ , and this is possible only by diffusion.

However, at the moment of immersion, there is no iron concentration gradient in this layer, and thus no possibility of transporting the flux,  $J$ , of iron injected by the corrosion. The iron produced therefore remains at the metal surface, where its concentration rises rapidly, so that a gradient is gradually established, leading to a flux of iron in the boundary layer (Fig. 1). This process obviously obeys Fick's two laws

$$\begin{cases} J = -D \text{grad Fe} & (2) \\ \frac{\partial \text{Fe}}{\partial t} = -\text{div } J = D \frac{d^2 \text{Fe}}{dx^2} & (3a) \end{cases}$$

with the following two boundary conditions

$$\begin{cases} J(x = d_0, t) = -J_0 = -K v_0 & (4a) \\ \text{Fe}(0, t) = \text{Fe}(x, 0) = 0 & (5a) \end{cases}$$

where  $\text{Fe}(x, t)$  is the concentration of iron in the liquid, expressed in  $\text{meq l}^{-1}$ ,  $J$  is the flux of iron, in  $(\text{meq l}^{-1})(\text{cm s}^{-1})$ , ( $K = 10^{-3}$ , from Equation 1b), and  $D$  is the diffusion coefficient of iron in  $\text{cm}^2 \text{s}^{-1}$ . Equation 5 signifies that, compared to the saturation concentration of iron,  $\text{Fe}_{s_0}$  [5], the mean content in the corrosive medium is generally negligible.

### 2.2.2. Iron enrichment at the surface of the liquid phase

If a dynamic equilibrium can be attained between the corrosion and diffusion fluxes, without anywhere exceeding the solubility limit of the iron ions, the steady state will correspond to a constant gradient and to an iron concentration in the liquid at the surface of the steel given by

$$\begin{aligned} \text{Fe}_0 &= \frac{d_0 J_0}{D} \\ &= d_0 \frac{K v_0}{D} \end{aligned} \quad (6)$$

The transient states can be expressed simply in dimensionless reduced coordinates  $X = x/d_0$ ,  $C = \text{Fe}/\text{Fe}_0$  and  $\tau = Dt/d_0^2$ . Fick's law (Equation 3) and the boundary conditions (Equations 4 and 5) can be written

$$\frac{\partial C}{\partial \tau} = \frac{d^2 C}{dX^2} \quad (3b)$$

$$\frac{dC}{dX}(1, \tau) = 1 \quad (4b)$$

$$\begin{aligned} C(0, \tau) &= C(X, 0) \\ &= 0 \end{aligned} \quad (5b)$$

In these reduced coordinates, the function  $C(X, \tau)$  is represented by a series of curves which are independent of the experimental data, and can be tabulated once and for all (Fig. 2). Returning to real coordinates, the variation of the distribution of iron in the boundary diffusion layer can thus be written

$$\begin{aligned} \text{Fe}(x, t) (\text{meq l}^{-1}) \\ &= 10^{-3} \frac{d_0}{D} v_0 (\text{mm/yr}) C\left(\frac{x}{d_0}, \frac{D}{d_0^2} t\right) \end{aligned} \quad (7)$$

where  $v_0$  is the initial corrosion rate of the steel.

In summary, as long as the solubility limit of the iron ions has not been reached, there is an iron enrichment in the solution, given in practical units by

$$\begin{aligned} \text{Fe}_0 (\text{meq l}^{-1}) &= \text{Fe}(d_0, \infty) \\ &= 10^{-7} \frac{d_0 (\mu\text{m})}{D (\text{cm}^2 \text{s}^{-1})} v_0 (\text{mm/yr}) \end{aligned} \quad (8)$$

For typical values  $v_0 = 1 \text{ mm/yr}$ ,  $D = 10^{-6} \text{ cm}^2 \text{s}^{-1}$  and  $d = 50 \mu\text{m}$  (in a stagnant medium), it is seen that the iron enrichment corresponds to a concentration  $\text{Fe}_0$  of  $5 \text{ meq l}^{-1}$ , i.e.  $125 \text{ mg l}^{-1}$ , which is far from negligible. If  $\text{Fe}_0$  is nevertheless lower than the local saturation value  $\text{Fe}_s$ , the steel remains bare indefinitely, and the real corrosivity of the medium is very close to its potential corrosivity.

### 2.2.3. Time to set up the steady state diffusion regime

The time necessary to set up this steady state condition is very short. For example, Fig. 2 shows that the two upper curves  $C(X, \tau)$  correspond to reduced times of 0.8 and 1.5. The steady state diffusion regime in the liquid phase is thus practically attained for reduced times of about 1, i.e. for real times  $\sim d_0^2/D$ . About 25 s is therefore sufficient in a stagnant medium ( $d_0 \sim 50 \mu\text{m}$ ), and less than 1 s as soon as the medium is agitated ( $d_0 < 10 \mu\text{m}$ ).

On the timescale of corrosion exposures, it can therefore be considered that a steady state corrosion and diffusion regime is set up on the bare metal practically instantaneously.

## 2.3. Precipitation of a corrosion deposit

### 2.3.1. Incubation time for precipitation

If, contrary to the preceding case,  $\text{Fe}(x, t)$  manages to attain or sufficiently exceed  $\text{Fe}_s$ , solid corrosion products will be precipitated. This precipitation will begin at the point where the concentration is highest, i.e. on the metal itself.

Because  $\text{Fe}_s$  is less than  $\text{Fe}_0$ , the incubation time for precipitation is even shorter than the time taken to set up the steady state on the bare metal. Thus, if a corrosion deposit is able to form, the precipitation of corrosion products starts almost instantaneously.

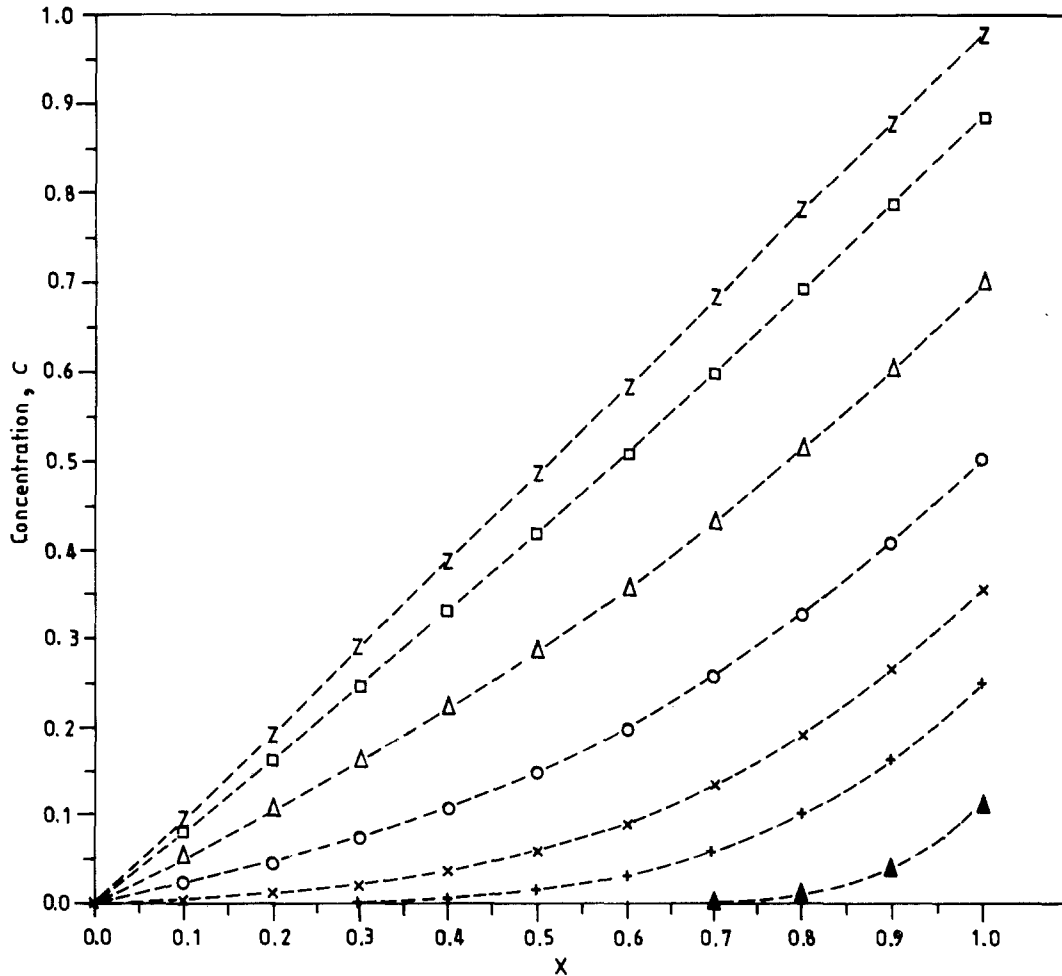


Figure 2 Build-up of an iron concentration gradient at the surface of a corroding metal. Curves of Fig. 1 in reduced coordinates  $C(X, \tau)$ , with  $C = \text{Fe}/\text{Fe}_0$ ,  $X = x/d_0$  and  $\tau = D/d_0^2 t$ .  $\tau$ : (▲) 0.01, (×) 0.10, (△) 0.40, (Z) 1.50, (+) 0.05, (○) 0.20, (□) 0.80.

### 2.3.2. Diffusion transients

Subsequently, the thickness  $d$  of the boundary diffusion layer rises with increasing deposit thickness; the corrosion rate,  $v$ , falls (possibly), and part of the flux of iron is drawn off to feed the deposit build-up.

Such a diffusion transient cannot be modelled simply. Nevertheless, it can be attempted to decompose the phenomena and to evaluate the times necessary. For example, Equations 7 and 8 could be rewritten with a corrosion rate,  $v$ , equal to the real final corrosivity under a stable deposit, a thickness  $d$  of the boundary diffusion layer equal to the sum of  $d_0$  and the final deposit thickness, and a final iron surface enrichment equal to the local saturation concentration  $\text{Fe}_s$ . These new equations correspond to the diffusion through a chemically inert porous scale, with the same protective properties as the final deposit, but already present at time  $t_0$ . If it were possible to interrupt a stabilized corrosion test, to rinse and dry the specimen without altering the deposit, and then to re-immerses it, the stationary diffusion regime would be set up in the same time as for Equations 7 and 8, i.e. a reduced time of the order of 1 s. However, even for thick deposits, the time  $t = d^2/D$  remains short,  $\sim 2$  min for 0.1 mm, and scarcely 3 h even for 1 mm.

Consequently, on the timescale observed experimentally for the stabilization of corrosion regimes

with deposit formation, the time required to set up the diffusion regime in the liquid phase is quite negligible: on this scale, diffusion in the liquid phase is a rapid phenomenon, which adapts itself permanently to the thickness of the porous solid deposit. Therefore, the process which controls the time to stabilize the deposit can only be the precipitation itself.

### 2.3.3. Precipitation transients

Consider now the material balance involved in the precipitation. The iron which serves to construct the deposit is provided entirely by the iron taken into solution by the corrosion. In effect, at the temperatures encountered in aqueous corrosion, diffusion in the solid state is negligible [7], so that the mechanisms observed in high-temperature corrosion, involving solid-state transport [1], are not transposable here. Deposit formation thus necessarily includes a stage in which  $\text{Fe}^{2+}$  ions are taken into solution, followed by precipitation.

Now, the ratio,  $R$ , between the molar volume of iron in the metal and in the deposit compound is typically of the order of 3 (4.3 for  $\text{FeCO}_3$ ; 2.6 and 3.4 for  $\text{FeS}$  and  $\text{FeS}_2$ ; 2.1 for  $\text{Fe}_3\text{O}_4$  [8]). Thus, to form a 0.1 mm siderite deposit ( $\text{FeCO}_3$ ), it is necessary to corrode

0.023 mm of steel, which, even with an initial rate of 1 mm/yr, requires at least 8 days.

Furthermore, during build-up of the deposit, the iron theoretically continues to be discharged into the external medium, by diffusion in the liquid which permeates the pores. However, the maximum iron content is limited to the saturation level  $Fe_s$ , and can no longer attain the value  $Fe_0$  defined for the steady state on bare metal (Equation 6). If  $Fe_0$  is very much greater than  $Fe_s$ , it can be seen that, as long as the corrosion rate remains close to the potential corrosivity  $v_0$ , or higher than the final real corrosivity, or at least, as long as  $Fe_0$  and  $Fe_s$  vary as the deposit grows so as to maintain a large difference between them ( $Fe_0 \gg Fe_s$ ), the fraction of the iron discharged to the external medium remains perfectly negligible compared to the overall production of corrosion products. In other words, as long as the deposit has not become protective, almost all of the corroded iron remains trapped within it in the form of solid corrosion products. In relative terms, during the deposit build-up stage, there is no significant loss of iron to the external corrosive medium. Consequently, the time required to establish the deposit is practically that needed to corrode the corresponding amount of corrosion products.

Unfortunately, it is impossible to model the variation in corrosion rate during the precipitation transient. In effect, this rate stays constant as long as it is controlled by an activation polarization, and subsequently varies with  $1/d$  if a diffusion polarisation is set up. For lack of anything better, an average value will therefore be taken between the initial potential corrosivity,  $v_0$ , and the final real corrosivity,  $v$ . The time,  $t$ , required to form a protective deposit of thickness,  $e$ , is then given by

$$t = \frac{2e}{R(v + v_0)} \quad (9)$$

#### 2.3.4. Practical consequences

**2.3.4.1. Detection of deposit formation.** According to Equation 9, for an initial corrosion rate  $v_0 = 10$  mm/yr, a highly protective deposit ( $v \ll v_0$ ) of thickness  $e = 0.1$  mm, and a molar volume ratio with respect to the metal of  $R = 4.3$  (e.g.  $FeCO_3$  under 3 bar  $CO_2$  at 60 °C [4]), the deposit build-up and the stabilization of the corrosion rate will take about 1.7 days. This time will obviously be greater for higher final deposit thicknesses and lower initial corrosion rates. In the above example, for  $v_0 = 1$  mm/yr, more than 2 weeks would be required to form and stabilize the deposit.

Thus, if the initial corrosion rate is limited, and if the deposit becomes protective only for fairly large thicknesses, the possibility of deposit formation can remain totally undetected in electrochemical tests of short duration [4]. When performing such tests, it is obviously important to control carefully all factors likely to influence or modify the solubility of the corrosion deposits [5].

**2.3.4.2. Profuse deposits.** It will be seen below that

some deposits can remain very slightly protective, even for large thicknesses. It is also possible to imagine that certain deposits could be so unprotective that they are unable to become stabilized. Such deposits would therefore never stop growing. Consequently, a certain, even major, proportion of the iron corroded remains trapped in this type of deposit. Because the latter occupies a volume greater than that of the metal from which it has formed, such unstabilized deposits are therefore profuse.

The comparison between the molar volume ratio for iron,  $R$ , and the effective ratio,  $R^*$ , for the profuse deposit then gives an overall measurement of the deviation from equilibrium.

Profuse deposits of this sort are effectively observed in well bottoms at LACQ [9], and in all cases of heavy general (or local) corrosion under  $H_2S$  pressure [10–12]. The ratio  $R^*$  is then about 3, compared to  $R$  values of 2.6–3.4 for the iron sulphides. This indicates that the corrosion rate under the deposit stays considerably higher than the value needed to stabilize it. It also signifies that almost all of the corroded iron has remained in the deposit.

#### 2.4. Sensitivity of the corrosion regime to environmental conditions

From the above considerations, it results that, if the quantitative parameters are appropriate, variations in environmental conditions can cause the metal to corrode either with or without deposit formation. Because the resulting corrosion rates are very different, the technological interest of modelling is immediately obvious.

Apart from the temperature, Equation 8 shows that the presence or absence of corrosion deposits depends basically on only three parameters; the potential corrosivity, the degree of turbulence and the solubility of iron.

##### 2.4.1. Potential corrosivity

For any given set of conditions, a certain minimum potential corrosivity is necessary for deposit formation (Equation 8). Because the precipitation may lower the corrosion rate, the variation of the real corrosivity as a function of the potential corrosivity will have the form indicated in Fig. 3. This somewhat paradoxical behaviour shows all the characteristic features of the passivation process [6], where it is often necessary to exceed a relatively high virtual corrosivity threshold in order to obtain finally an acceptable residual corrosivity.

The expression “passivation by the corrosion products”, often employed by corrosion engineers, is thus revealed to be more valid than it might appear at first sight, with striking similarities between the patinas or barrier layers and passive films [1].

##### 2.4.2. Turbulence

The potential corrosivity necessary for the formation of a protective layer increases with decreasing boundary layer thickness (Equation 8), and therefore with

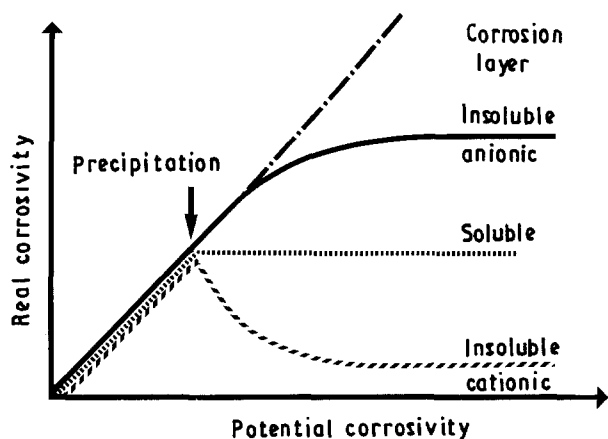


Figure 3 Various possible forms of relationship between real and potential corrosivity.

rising turbulence. For suitable values, increased turbulence can thus cause a transformation from deposit formation to deposit-free corrosion, resulting in higher real corrosivity.

Similarly, if the initially high potential corrosivity is due to heavy turbulence (diffusion polarization), the protective effect of the deposit will be observed from the very start of precipitation, thus increasing the time required to generate the volume of corrosion products necessary to set up and stabilize the deposit. This is obviously another potential source of spurious weight-loss measurements in laboratory experiments. However, a laboratory test medium should never be totally stagnant, unless complete stagnancy is one of the specific service conditions to be studied.

#### 2.4.3. The solubility of iron

All that has just been said concerning the critical potential corrosivity threshold and erosion-corrosion naturally depends on the local solubility of iron. A high solubility increases the critical potential corrosivity required for pseudo-passivity, at the same time decreasing the turbulence and erosion-corrosion thresholds.

Nevertheless, it is essential to understand fully this concept of local iron solubility. The latter depends first of all on the anion  $X^{n-}$  from which the salt or hydroxide is formed, and on the corresponding solubility limit  $K_s$ . The saturation concentration in iron [5],  $Fe_s$ , will therefore be given by the solubility product of the precipitating compound

$$Fe_s^n \cdot [X^{n-}]^2 = K_s^q \quad (10)$$

with  $q = 1$  if  $n \neq 2$ , and  $q = 2$  if  $n = 2$ . In this equation,  $[X^{n-}]$  may possibly depend on the local pH, if it is the anion of a polyacid, such as  $H_2CO_3$ ,  $H_2S$  [5] or  $H_2SO_4$ , and if the pH is close to the pK of the acid. Finally, like  $H^+$ ,  $X^{n-}$  can be implicated in the oxidizing power of the medium. If the potential corrosivity is itself under diffusion control, it is then possible to have a gradient in both  $X^{n-}$  and pH at the liquid surface.

The local solubility of iron is consequently not necessarily simple to model, and diffusional models of local equilibria must therefore be developed, taking

into account all of the transport phenomena and all of the physical-chemical interactions involved in the system. However, the technological repercussions of such models are sufficiently rewarding to justify their construction, in spite of their complexity. Indeed, such models for the solubility of iron must form the heart of any overall model for describing the corrosion rate of a metal beneath a deposit.

#### 2.5. The cause and effect of corrosion deposits

The precipitation of corrosion products occurs initially because the diffusion flux in the liquid phase is unable to remove all the iron injected by the corrosion, even with the maximum possible concentration gradient, i.e. between the saturation concentration of iron at the metal surface and a zero content in the convective zone.

Experience then shows that the growth and stabilization of a corrosion deposit is the solution adopted by the system for ensuring the rate-controlling dynamic equilibrium between the diffusion flux of iron and that of  $H^+$ . Consequently, the role of the deposit cannot be restricted to that of a simple inert obstacle at the metal surface, because the two fluxes would be modified in the same proportions, and it would not be possible to attain a steady state regime.

The same is true [7] for any purely geometrical effect, such as an increase in the diffusion path (due to the thickness of the deposit to be penetrated), or a variation in the effective area open to diffusion (e.g. in certain special porous structures).

The effect of a corrosion deposit cannot therefore be reduced to that of a simple porous layer, acting merely as a diffusion barrier. In fact, the fundamental role of the deposit is not so much to impede exchanges, as to balance the rate of creation of iron ions by corrosion and their rate of dispersion in the corrosive medium. Theoretically, such an equilibrium can occur with or without the permanent passage via a precipitation stage. In both cases, the effect of the deposit is to increase the diffusional flux of iron compared to the corrosion rate. This can be achieved either by increasing the former or by decreasing the latter, or by varying both to a different extent. All of these cases will be examined in turn.

### 3. Corrosion beneath a deposit

The mechanism of corrosion beneath a stabilized deposit which apparently most resembles the corrosion of bare metal is obviously pure direct formation. In effect, as on the bare metal, precipitation no longer occurs during the steady state regime, and all the transport Equations 1-5 can be employed without modification. For the sake of simplicity, we shall therefore start by examining this mechanism.

From the outset, it can be stated that the pure direct formation mechanism is based on the implied hypothesis that some process selectively impedes the corrosion rate, enabling iron enrichment to be restricted to its local solubility limit. Numerous such processes

can be envisaged. They necessarily depend on the detailed physical chemistry of the local corrosive medium [5], and therefore on each type of corrosion. The discussion will be limited to the case of an acidic medium ( $H^+ > OH^-$  at all points), where the only (or principal) oxidizing agent is the  $H^+$  ion.

### 3.1. Necessity for a diffusion potential across the deposit

In the steady state, when a transient precipitation stage has led to the formation of a stable deposit, according to the present hypothesis, precipitation no longer occurs in the system. This means that the solubility limit of the corrosion products must never be exceeded in the liquid within the porosities. Moreover, in this stationary state, and in this particular liquid, the  $Fe^{2+}$  and  $H^+$  fluxes are in equilibrium. There is, therefore, no transport of electric current. Furthermore, all the fluxes are conservative ( $\partial C/\partial t = 0$  in Equation 3). Consequently, the only fluxes which can subsist are those of the reacting species  $Fe^{2+}$  and  $H^+$  (Equation 2). All other fluxes cancel out in the steady state. In particular, there can be no stable flux of inert ions, such as  $Na^+$  or  $Cl^-$ , or even of the  $X^{n-}$  anion initially involved in the deposit (all precipitation has stopped).

Finally, the electrical neutrality of the interstitial liquid must be everywhere ensured. However, because of the difference between the respective diffusion coefficients  $D$  and  $D'$  for  $Fe^{2+}$  and  $H^+$  ( $D < D'$ ), equal fluxes imply different gradients. There is, therefore, an overall spatial variation of the sum ( $Fe + H$ ), which must be balanced by a parallel change in the total anion population, or by an inverse variation in that of all the other cations. In other words, fluxless concentration gradients must exist.

Such a situation is quite possible, all that is required being the existence of other driving forces for diffusion [7]. Under isothermal conditions, and in the absence of a magnetic field, the only possibility is the local presence in the medium of a non-zero electric field [7].

By analogy with reference ([7], p. 1037),  $V(x)$  will be termed the "diffusion potential". This potential has basically the same origin as all the junction potentials well known to electrochemists, except that it is not the differences in concentration which must be maintained stable, but rather the diffusion fluxes of the species involved in the corrosion reactions.

If the electric field is not uniformly zero, there will be a potential difference,  $V$ , within the liquid phase, between the convective zone of the corrosive medium and the surface of the liquid in contact with the metal.

Across what will nevertheless still be termed the "diffusion layer", the transport of ions in solution does not therefore occur by simple diffusion, but by diffusion in an electric field, i.e. a combination of "chemical" diffusion and electromigration. Fick's law [1] then becomes the generalized Equation 7

$$J = -D(\text{grad } c \pm nc \frac{e}{kt} \text{grad } V) \quad (11)$$

where  $J$  and  $c$  are, respectively, the flux and the concentration of the ion ( $\text{meq l}^{-1}$ ),  $\pm n$  its valency,  $e$  the unit electronic charge, and  $k$  Boltzmann's constant. It would have been equally possible to use more conventional electrochemical notations, such as the Faraday ( $F$ ) or the perfect gas constant ( $R(e/kT = F/RT)$ ). However, the present notation has the advantage that at room temperature ( $T = 293 \text{ K}$ ), the value of  $kT$  is exactly 25 meV.

In the absence of flux ( $J = 0$  in Equation 11), a diffusion potential of only 25 mV, very small by corrosion standards, would therefore enable the stabilization of a difference in concentration of  $n/2.3$  decades for ions of valency  $n$ , which is quite appreciable. For the same reason, these variations in concentration can be highly localized. In effect, for a constant electric field, grad  $V$ , the spatial distribution of an immobile ion, is given by

$$c(x) = c(0) \exp\left(-x \frac{\pm ne \text{grad } V}{kT}\right) \quad (12)$$

For a diffusion potential of 1 mV, the relative variation in  $c$  is thus  $4n\%$ .

With such powerful effects, the diffusion potentials can only be of the order of a few millivolts, i.e. very low values compared to the variations encountered in the corrosion potentials themselves. This explains why, until now, these diffusion potentials have not been detected experimentally. Nevertheless, they are probably responsible for the drifts of a few millivolts, or even tens of millivolts, observed after immersion of new specimens.

In effect, it will be noted at this point that the creation of the diffusion potential is not due fundamentally to the presence of a deposit, but to the existence of a steady state. On bare metal, corroding in the stationary regime, a diffusion potential thus already exists. The treatments developed in Section 2 therefore incorporate the implicit approximation that the diffusion potential is negligible. Indeed, on bare metal, the small thickness,  $d$ , of the limiting diffusion layer prevents the diffusion potential from reaching significant levels. It will be seen below that the specific role of a deposit is, in fact, to thicken this diffusion layer, by adding the deposit thickness to that of the natural layer,  $d_0$ . In this way, it increases the range of action of the local electric field, which in turn raises the diffusion potential.

Given the complexity of the diffusion potential, and the strength of its effects, the question is therefore whether this diffusion in an electric field can achieve what the elementary chemical diffusion is unable to do, that is, to establish an equilibrium between the flux of iron transported away from the surface and that injected due to the corrosion, i.e. to balance the  $Fe^{2+}$  and  $H^+$  fluxes in the deposit.

### 3.2. Evaluation of the diffusion potential

Because a diffusion potential,  $V(x)$ , exists across the deposit, the distribution and the fluxes of  $Fe^{2+}$ ,  $H^+$ , and of the precipitable anion  $X^{n-}$  are controlled by

generalized Fick's equations of the type (Equation 11)

$$\begin{aligned} \text{grad Fe} + 2\text{Fe} \frac{e}{kT} \text{grad } V &= + \frac{J}{D} \\ &= + K \frac{v}{D} \end{aligned} \quad (13)$$

$$\begin{aligned} \text{grad H} + \text{H} \frac{e}{kT} \text{grad } V &= - \frac{J}{D'} \\ &= - \frac{Kv}{D'} \end{aligned} \quad (14)$$

$$\text{grad X} - nX \frac{e}{kT} \text{grad } V = 0 \quad (15)$$

where  $v$  is now the corrosion rate at the bottom of the pores. Furthermore, at any point, the electrical neutrality requirement gives

$$\text{H} + \text{Fe} + \sum K_i = \sum A_j \quad (16)$$

where  $A_j$  represents the  $A_j^{n-}$  anion concentrations ( $\text{meq l}^{-1}$ ), and  $K_i$  all cations other than  $\text{H}^+$  and  $\text{Fe}^{2+}$ . Differentiating Equation 16, then applying Equation 15 to all the  $K_i$  and  $A_j$  gives

$$\begin{aligned} \text{grad H} + \text{grad Fe} &= \text{grad} \left( \sum_j A_j - \sum_j K_i \right) \\ &= \frac{e}{kT} \text{grad } V \left( \sum_j n_j A_j + \sum_i n_i K_i \right) \end{aligned} \quad (17)$$

which can then be inserted into Equations 13 and 14

$$\frac{e}{kT} \text{grad } V = \frac{Kv}{2I} \left( \frac{1}{D} - \frac{1}{D'} \right) \quad (18)$$

where  $I = 1/2(\text{H} + 2\text{Fe} + \sum_j n_j A_j + \sum_i n_i K_i)$  is the local ionic strength.

In terms of the iron enrichment  $\text{Fe}_0$  necessary to remove the flux produced by corrosion of the bare metal (Equation 6), Equation 18 can also be written

$$\frac{e}{kT} \text{grad } V = \frac{r}{d_0} \frac{\text{Fe}_0}{2I} \left( 1 - \frac{D}{D'} \right) \quad (19)$$

where  $r = v/v_0$  is the ratio between the potential corrosivity,  $v_0$ , and the dissolution rate,  $v$ , at the bottom of the pores.

The relative values of  $D$  and  $D'$  depend essentially on the temperature. If the diffusion coefficient of  $\text{Fe}^{2+}$  is assimilated to that of another bivalent ion such as  $\text{Ca}^{2+}$  ( $D$  is practically the same for all bivalent ions), it is found that  $D/D'$  varies from 1/12 between 10 and 50 °C to 1/4 at about 150 °C [8].

With the sign convention chosen (Fig. 1), the electric field,  $-\text{grad } V$ , corresponding to the diffusion potential is always negative. It attracts the anions towards the metal and repulses the cations. It thus participates in the removal of the iron generated by the corrosion, and at the same time reduces the amount produced, by impeding the supply of  $\text{H}^+$ . The diffusion potential therefore acts in the direction required to balance the flux of iron produced with that which can be removed by liquid-phase transport. However, the diffusion potential simultaneously promotes an enrichment in precipitable anion in contact with the metal, leading

to a decrease in the local solubility of iron. It is therefore impossible to predict whether the diffusion potential will really provide a solution to the problem or whether, on the contrary, the latter may even become more difficult to overcome.

Moreover, the absolute value of the diffusion potential depends strongly on the local salinity (Equations 18 and 19). Thus, for a 100  $\mu\text{m}$  deposit and a corrosion rate of 1 mm/yr, the value would be 10 mV for a condensation water with an ionic strength of 1  $\text{meq l}^{-1}$ , and only 0.1 mV for water with a salt concentration  $I = 1000 \text{ meq l}^{-1}$ . Although the diffusion potential is apparently always fairly weak, it can nevertheless exert a strong influence on the transport and the equilibria of the different species present.

### 3.3. Influence of the diffusion potential

The equations describing the profiles of the three principal species  $\text{Fe}^{2+}$ ,  $\text{H}^+$  and  $\text{X}^{n-}$  can be obtained directly by replacing  $\text{grad } V$  in Equations 13–15 by the value derived from Equation 18

$$\text{grad H} = - \frac{Kv}{D'} \left[ 1 + \frac{\text{H}}{2I} \left( \frac{D'}{D} - 1 \right) \right] \quad (20)$$

$$\text{grad Fe} = \frac{Kv}{D} \left[ 1 - \frac{\text{Fe}}{I} \left( 1 - \frac{D}{D'} \right) \right] \quad (21)$$

$$\text{grad X} = n \frac{X}{2I} Kv \left( \frac{1}{D} - \frac{1}{D'} \right) \quad (22)$$

In the expression inside the brackets in Equations 20 and 22, the first term, 1, represents transport by chemical diffusion, while the second term, involving H or Fe, corresponds to the electromigration contribution. Equations 20 and 21 thus confirm that to transport a given flux,  $Kv$ , in the presence of a diffusion potential, the  $\text{H}^+$  gradient must be higher and that for  $\text{Fe}^{2+}$  lower.

#### 3.3.1. Influence on the profile and transport of $\text{H}^+$

Equation 20 shows first of all that there is a critical ratio between the acidity H and the ionic strength  $I$ , below which  $\text{H}^+$  is transported solely by simple chemical diffusion, and above which the supply of  $\text{H}^+$  to the corrosion reaction involves electromigration due to the diffusion potential. The corresponding critical pH is given by

$$\text{pH}_c = \log \frac{D'/D - 1}{2} - \log I \quad (23)$$

$\text{pH}_c \simeq 0.7$  (at 25 °C) to 0.2 (at 150 °C)  $-\log I (\text{eq l}^{-1})$ . This limit will therefore separate media which are "more saline than acid", with  $\text{H}^+$  diffusion, from those which are "more acid than saline", with electromigration. Moreover, it will be noticed that the saline/acid transition occurs at a pH of about 3.5 for  $I = 1 \text{ meq l}^{-1}$ , and this can have significant consequences in the case of high-pressure corrosion by the sour gases  $\text{CO}_2$  or  $\text{H}_2\text{S}$  [5].

Finally, if the medium is a concentrated acid,  $\text{H}^+$  will be the major cation, and the major anion will also



be monovalent (first dissociation of the acid), so that  $H = \frac{1}{2}I$ . Equation 20 can thus be written

$$\text{grad } H = -\frac{Kv}{D'} \left[ 1 + \left( \frac{H}{2I} \text{ or } \frac{1}{4} \right) \left( \frac{D'}{D} - 1 \right) \right] \quad (24)$$

Integration of Equation 24 therefore yields the three asymptotic  $H^+$  profiles

(i) saline medium

$$H(x) \simeq H_0 - \frac{Kv}{D'} x \quad (25)$$

(ii) dilute acid medium

$$H(x) \simeq H_0 \exp \left[ -\frac{Kv}{2I} \left( \frac{1}{D} - \frac{1}{D'} \right) x \right] \quad (26)$$

(iii) concentrated acid medium

$$H(x) \simeq H_0 - \frac{Kv}{4} \left( \frac{1}{D} + \frac{3}{D'} \right) x \quad (27)$$

In the two cases of acid media, it is obvious that for transport polarization, Equations 25 and 27 correspond only to the outer region of the diffusion layer, which is still relatively little modified. Further inwards, the depletion in  $H^+$  and the enrichment in iron will lead to transitions towards the more saline and less acid cases. There is no analytical solution for this transition for concentrated acid media, i.e. between Equations 27 and 26. In contrast, for saline and dilute acid media, the exact solution of Equation 20 or 24 at all points in the deposit thickness can be written

$$H(x) = \left( H_0 + \frac{2ID/D'}{1-D/D'} \right) \exp \left[ \frac{Kv}{2I} \left( \frac{1}{D} - \frac{1}{D'} \right) x \right] - 2 \frac{ID/D'}{1-D/D'} \quad (28)$$

By an expansion limited to the first order in  $I/H_0$  or in  $Kv/I$ , it can easily be verified that Equation 28 integrates the two asymptotic forms, Equations 25

and 26. It can also be verified that the curves corresponding to Equations 28 and 25 become parallel when  $H^+$  exhaustion eventually renders electromigration effects negligible (Fig. 4a).

On the whole, compared to the elementary chemical diffusion model, which remains valid in saline solutions, the influence of electromigration in acid media is simply to increase the  $H^+$  gradient in the outside of the diffusion layer (Fig. 4a), the maximum relative effect being obtained in concentrated acids. However, depending on the value of the  $D/D'$  ratio [8], this maximum effect is only a factor of 4 at room temperature, and even falls to a factor of 2 at about 150°C.

If the thickness of the diffusion layer is sufficient to induce transport polarization (total depletion of  $H^+$  at the metal surface), the eventual arrival of  $H^+$  at the metal surface nevertheless still continues to occur in all cases solely by chemical diffusion (Fig. 4a). By shifting the  $H^+$  profiles, the role of electromigration in an acid medium is simply to reduce the minimum boundary layer thickness required to induce transport polarization (arrows in Fig. 4a).

By promoting a boundary-layer thickness,  $d$ , greater than the natural thickness,  $d_0$ , a corrosion deposit can thus lead to an increase in transport polarization (Fig. 4b). This is, of course, only a possibility, and is by no means a necessity. Indeed, complete transport polarization occurs in the deposit for  $H(d) = 0$ . From Equation 28, the maximum pore tip dissolution rate is then

$$v = \frac{1}{K} \frac{2I}{d} \frac{1}{1/D - 1/D'} \ln \left[ 1 + \frac{H_0(1 - D/D')}{2ID/D'} \right] \quad (29)$$

For this same corrosion rate,  $v$ , partial transport polarization, defined by  $H(d_0)$ , would occur on the bare metal (Fig. 4b). For all rates less than  $v$ , the necessary  $H^+$  fluxes could thus be ensured both on the bare metal and under a deposit. There would then be no reduction in dissolution rate in the pores.

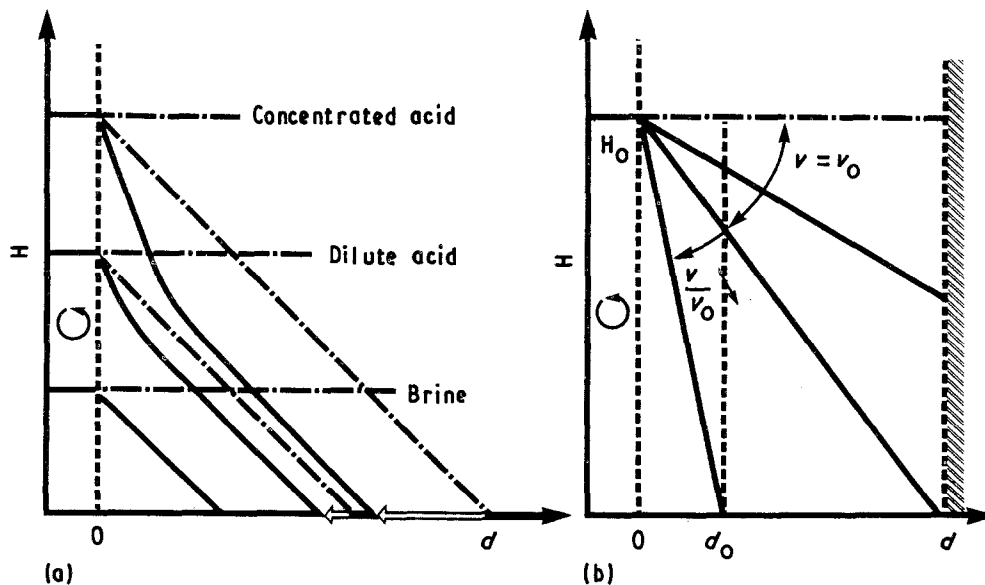


Figure 4  $H^+$  concentration profile in a corrosion deposit. (a) Influence of electromigration in dilute or concentrated acid media; (b) effect of an increase ( $d_0 \rightarrow d$ ) in the thickness of the diffusion layer, on the possible reduction in the corrosion rate,  $v$ , beneath a deposit.

Conversely, for all rates  $v_0 > v$ , there will be a protective effect due to the increase in transport polarization. This effect will be a maximum if the transport polarization is already complete on the bare metal ( $H(d_0) = 0$ ). In this case, Equation 29 then gives

$$\begin{aligned} r &= \frac{v}{v_0} \\ &= \frac{d_0}{d} \end{aligned} \quad (30)$$

In saline or acid media, whatever the relative extent of electromigration, and in spite of the complexity of the exact concentration profiles, it can thus be seen that the maximum inhibition due to the deposit is strictly the same as in the elementary diffusion model (Equation 25 and Fig. 4b).

Finally, it is evident that, whatever the bare metal corrosion rate, a deposit can be protective provided that it is sufficiently thick. However, the degree of protection will be greater, or the minimum deposit thickness smaller, the more advanced is the transport polarization on the bare metal itself.

### 3.3.2. Influence on the profile and transport of $Fe^{2+}$

As with  $H^+$ , two domains will be distinguished, corresponding, respectively, to iron transport either by diffusion alone or by a combination of diffusion and electromigration.

At the edge of the convective zone, iron is necessarily a minority constituent of the chemical salinity. The iron concentration profile can therefore be obtained by integrating Equation 21 using Equations 18 and 19, with  $Fe \ll I_0$ . In this outer region of the diffusion layer, the iron will thus be transported essentially by diffusion

$$\begin{aligned} Fe(x) &= \frac{Kv}{D} x \\ &= r Fe_0 \frac{x}{d_0} \end{aligned} \quad (31)$$

Because the iron content increases on approaching the metal, it can eventually become the major constituent of the local salinity. In this case

$$Fe = \alpha I \quad (32)$$

with  $\alpha = 2/3, 1/2$  or  $2/5$ , depending on whether the major local anion is mono-, bi- or trivalent. Equation 21 then becomes

$$Fe(x) = \frac{Kv}{D} (1 - \alpha^*) x + cte \quad (33a)$$

with  $\alpha^* = \alpha(1 - D/D')$ .

In chloride or sulphate containing media, the iron gradient in contact with the metal can therefore be reduced to a third or a half of its value in the outer part of the diffusion layer. In contact with the metal, two-thirds or half of the iron flux is then ensured by electromigration.

A precise linkage between the two asymptotic forms, Equations 31 and 33, would require complete numerical solution of the system of Equations 20–22 for all chemical species present. Nevertheless, for a saline or dilute acid medium, an approximate junction can be determined by equating the asymptotes themselves for the value  $Fe = \alpha I_0$  ( $I_0$  = ionic strength of the external corrosive medium). This value corresponds to a pure iron salt, of the same ionic strength as the external medium, and with the same relative anionic composition as the internal region of the deposit. From Equation 34 below, this value,  $\alpha I_0$ , effectively corresponds to a zone where the cations in the external medium represent no more than about 10% of the total cation concentration, the anions having been enriched by a ratio of  $\sim e$ , and the cations depleted by a ratio  $\sim 1/e$  (this would no longer be true in concentrated acids).

Equating Equations 31 and 33 for the value  $Fe = \alpha I_0$  enables the constant in Equation 33 to be determined

$$\begin{aligned} Fe(x) &= \frac{Kv}{D} (1 - \alpha^*) x + \alpha \alpha^* I_0 \\ &= r Fe_0 (1 - \alpha^*) \frac{x}{d_0} + \alpha \alpha^* I_0 \end{aligned} \quad (33b)$$

### 3.3.3. Influence on the profile of precipitable anion $X^{n-}$

In the outer zone where the ionic strength remains constant, integration of Equation 22 yields

$$\begin{aligned} X(x) &= X_0 \exp \left[ \frac{nKv}{2DI_0} \left( 1 - \frac{D}{D'} \right) x \right] \\ &= X_0 \exp \left[ \frac{nFe(x)}{2I_0} \left( 1 - \frac{D}{D'} \right) \right] \end{aligned} \quad (34)$$

In the inner region, Equation 22 can be combined with Equations 21 and 32 as follows

$$\frac{\text{grad } X}{X} = \frac{\alpha^*}{1 - \alpha^*} \frac{n \text{ grad } Fe}{2 Fe} \quad (35)$$

This gives:

$$X(x) = cte [Fe(x)]^{\frac{n \alpha^*}{2(1 - \alpha^*)}} \quad (36a)$$

The junction between the two asymptotic forms Equations 34 and 36, naturally occurs at the same point as that between Equations 31 and 33 (swing in the  $Fe/I$  ratio as  $Fe$  changes from a minor to the major cation). The constant in Equation 36 is therefore determined in the same manner, by equating Equations 34 and 36 for the value  $Fe = \alpha I_0$ , whence

$$X(x) = X_0 \exp \frac{n \alpha^*}{2} \left( \frac{Fe(x)}{\alpha I_0} \right)^{\frac{n \alpha^*}{2(1 - \alpha^*)}} \quad (36b)$$

It can be seen in particular from Equations 34 and 36 that the tendency for the corrosion deposit to concentrate the anions is greater, the higher is their valency. Compared to the external medium, the liquid within the deposit is thus not only more concentrated, but also enriched in bi- and trivalent anions.

### 3.3.4. Influence on the solubility product of the precipitable compound

By definition, the local solubility product  $P(X)$  of the compound  $Fe_nX_2$  is given by

$$[P(x)]^q = [Fe(x)]^n [X(x)]^2 \quad (37)$$

with  $q = 1$  for  $n \neq 2$ , and  $q = 2$  for  $n = 2$ .

In the outer region of the diffusion layer, the profile of  $P$  is obtained from Equations 31 and 34

$$\begin{aligned} [P(x)]^q &= X_0^2 [Fe(x)]^n \exp \left[ n \frac{Fe(x)}{I_0} \left( 1 - \frac{D}{D'} \right) \right] \\ &= X_0^2 \left( r Fe_0 \frac{x}{d_0} \right)^n \exp \left[ nr \frac{Fe_0}{I_0} \left( 1 - \frac{D}{D'} \right) \frac{x}{d_0} \right] \end{aligned} \quad (38)$$

Similarly, in the inner zone, the profile is obtained from Equations 33b and 36b

$$[P(x)]^q = X_0^2 \left( \alpha I_0 e^{2^*} \right)^n \left( \frac{Fe(x)}{\alpha I_0} \right)^{1-\alpha^*} \quad (39)$$

Now that the concentration profiles of the three species  $Fe^{2+}$ ,  $H^+$ , and  $X^{n-}$  are known, the scale formation and stabilization mechanisms can be considered.

### 3.4. Impossibility of a pure direct formation mechanism

It has been seen above that the presence of the diffusion potential is due, not to the existence of a deposit, but to that of a steady state. Equations 31–39 therefore apply equally well to corrosion of the bare metal (with  $0 < x < d_0$ ) as to that of metal beneath a deposit.

As in the elementary model, the metal thus remains bare as long as the solubility product  $P(d_0)$  is less than the solubility limit  $K_s$  (Equation 10). Consequently, it will be simpler to consider the saturation concentration of iron in the corrosive medium, defined as in Equation 10 by  $Fe_{s_0} \cdot X_0^2 = K_s^q$ . The concentration of iron is, in effect, the principal variable in the system, and  $Fe_{s_0}$  is virtually the "iron solubility limit" in the virgin corrosive medium.

Furthermore, the degree of saturation of the corrosive medium in  $Fe_nX_2$  can be defined as  $Fe/Fe_{s_0}$  [5], provided that the anion concentration  $X_0$  remains unchanged.

By considering  $Fe_{s_0}$ , two cases can be distinguished, depending on whether the solubility is low ( $Fe_{s_0} \ll \alpha I_0$ ) or high ( $Fe_{s_0} \gg \alpha I_0$ ). In fact, this iron solubility level depends not only on that of the  $Fe_nX_2$  salt, i.e. on the value of  $K_s$ , but also on the anion content  $X_0$  of the medium. It can even be said that, as regards deposit formation, this notion of iron solubility is practically independent of that of the solubility of the iron salt.

#### 3.4.1. Case of low iron solubility

Even when the solubility limit of iron is attained, iron still remains a minority cation in the local medium:  $Fe(x) < Fe_{s_0} \ll \alpha I_0$ . The diffusion layer is thus composed only of its outer zone, where the transport of

iron occurs essentially by chemical diffusion (Equation 31), and where the anion content  $X^{n-}$  is little modified (Equation 34). The solubility product is then given by Equation 38.

The metal therefore stays bare if  $P(d_0)$  remains less than  $K_s$ , so that

$$Fe_{s_0} \geq Fe_0 \exp \frac{Fe_0}{I_0} \left( 1 - \frac{D}{D'} \right) \simeq Fe_0 \quad (40)$$

The elementary diffusion model (Equation 9) was thus a good approximation in this case.

On the contrary, if Equation 40 cannot be satisfied, corrosion products will be precipitated in contact with the metal, and a deposit will grow by accumulation. This growth increases the thickness of the diffusion layer, and stops only if the solubility product  $P(d)$  manages to remain at the  $K_s$  level in contact with the metal, or if  $Fe(d)$  stays at the  $Fe_{s_0}$  level. Equation 38 therefore gives

$$Fe(d) = r Fe_0 \frac{d}{d_0} \exp \left[ r \frac{Fe_0}{I} \left( 1 - \frac{D}{D'} \right) \frac{d}{d_0} \right] \quad (41)$$

From Equation 30, it is known that  $r$  is always greater than  $d_0/d$ . If  $Fe_0$  were to exceed  $Fe_{s_0}$ , it would necessarily follow that  $Fe(d) \geq Fe_0 > Fe_{s_0}$ .

If the iron solubility limit is low, and if this limit is attained on the bare metal, local precipitation of corrosion products will continue indefinitely.

#### 3.4.2. Case of high iron solubility

The iron solubility limit is attained in a domain where iron is the majority cation in the medium. The solubility product is then given by Equation 39. Here again, in order for the precipitation of corrosion product to be able to stop,  $P(d)$  must be able to stay at the  $K_s$  level, so that Equation 39 leads to the condition

$$Fe(d) \leq \alpha I_0 \left( \frac{Fe_{s_0}}{\alpha I_0} \right)^{1-\alpha^*} \exp [ -\alpha^*(1-\alpha^*) ] \quad (42)$$

If  $Fe(d)$  in Equation 42 is replaced by the value derived from Equation 33b, this condition becomes

$$\begin{aligned} &\frac{rd}{d_0} (1 - \alpha^*) \frac{Fe_0}{\alpha I_0} + \alpha^* \\ &\leq \left( \frac{Fe_{s_0}}{\alpha I_0} \right)^{1-\alpha^*} \exp [ -\alpha^*(1-\alpha^*) ] \end{aligned} \quad (43)$$

For Equation 43 to be satisfied with  $rd/d_0 > 1$  (Equation 30),  $\alpha^* > 0$  (Equation 33), and  $\exp ( <0 ) < 1$ , it would be necessary for

$$\frac{Fe_0}{Fe_{s_0}} < \frac{\alpha I_0}{Fe_{s_0}} \quad (44)$$

However, the first term is  $> 1$  (precipitation on bare metal) and the second is  $< 1$  (high iron solubility limit). Conditions 42–44 are therefore impossible, and the precipitation of corrosion products initiated on bare metal cannot be stopped, whatever the thickness of the corrosion deposit.

#### 3.4.3. Summary

Whether the corrosive medium be saline or acid, and

whatever the additional transport polarization due to the corrosion deposit, the precipitation of corrosion products cannot be prevented by the presence of a deposit. The mechanism of direct deposit formation thus cannot exist in the pure state.

The fundamental reasons for this impossibility are relatively easy to illustrate in a simple diffusion model. If, on the bare metal, the potential corrosivity is already controlled by total transport polarization (Fig. 5a), then, although the restriction of the  $H^+$  and  $Fe^{2+}$  fluxes is a maximum, it is exactly the same for each species. Consequently, the iron concentration attained in contact with the metal remains strictly the same whatever the thickness of the deposit.

Conversely, if restriction is nonexistent (Fig. 5b), the concentration of iron in contact with the metal is much greater beneath a deposit than on the bare metal.

In all cases, while the electromigration certainly lowers the  $Fe(x)$  curve, it also has a similar, even greater, effect on that for  $Fe_s(x)$  (arrows in Fig. 5).

If  $Fe_0$  is already greater than  $Fe_{s_0}$  on bare metal, the supersaturation  $Fe(d)/Fe_s(d)$  is therefore always at least as high beneath a deposit, and can only be increased further if electromigration contributes to the overall transport.

In conclusion, the pure direct formation mechanism is impossible, and a certain degree of precipitation must necessarily exist at the metal–deposit interface.

### 3.5. The various consequences of precipitation

It has just been seen that, if a corrosion deposit forms, the kinetics of transport in the solution are unable, by themselves, to prevent precipitation from continuing at the pore tip. All of the previously established transport equations will therefore have to be modified,

starting with Equation 15. The latter must now reflect the existence of an overall flux of  $X^{n-}$  ions

$$J_X = -D'' \left( \text{grad } X - n X \frac{e}{kT} \text{grad } V \right) \quad (45)$$

where  $D''$  is the diffusion coefficient of the  $X^{n-}$  ion.

If the concentration  $X_0$  in the external corrosive medium is sufficiently small, the transport of  $X^{n-}$  ions between the external medium and the metal represents the slowest stage and is therefore the rate-controlling step in the overall precipitation process. The  $X^{n-}$  ions are then depleted in contact with the metal and the local iron solubility limit  $Fe_s(d)$  is greatly increased. The removal of iron can thus take place almost completely by liquid-phase transport, whatever the iron profile in Fig. 5. All the essential features of a direct deposit formation mechanism are thus united, in this case with anion control in the steady state. For short, this will be termed an “insoluble anionic deposit”.

Conversely, if the concentration  $X_0$  of the external medium is sufficiently high, precipitation is no longer limited by the supply of anions and its kinetics depend solely on the local degree of supersaturation in  $Fe_nX_2$  compound (the only consequence of the transformation from Equation 15 to Equation 45 is a modification in the value of the diffusion potential).

Depending on the supersaturation level required to trigger precipitation, the latter will occur in different places:

(a) for low supersaturations, the new solid must form on the existing deposit (seeding effect);

(b) on the contrary, for high supersaturations, the new solid forms on the metal (maximum supersaturation).

In the first case, the pores remain open. Corrosion and precipitation therefore continue permanently, at closely similar rates. Almost all of the corroded iron thus transits via the deposit, so that it is essentially

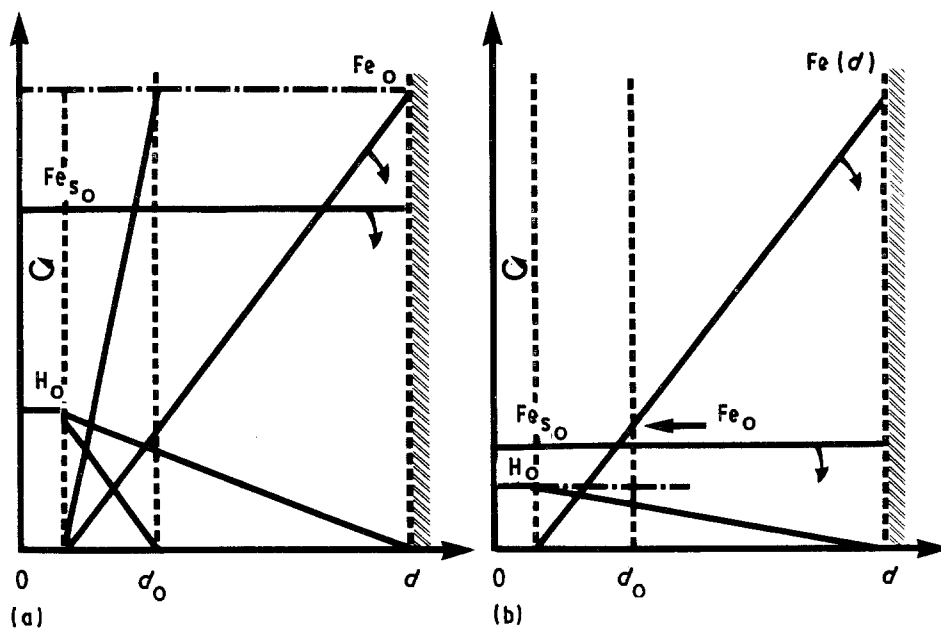


Figure 5 Impossibility of a pure direct precipitation mechanism. (a) Diffusion polarization on bare metal, maximum reduction in the corrosion rate, but  $Fe(d) = Fe_0 = \text{constant}$ ; (b) zero reduction,  $Fe(d) > Fe_0$ .

a precipitation–redissolution mechanism, and the term “soluble deposit” will be used for the sake of brevity.

In the second case (Fig. 6a), because the water no longer has access to the metal, the corrosion reaction is immediately impeded, until the elimination of iron by liquid-phase transport lowers its local concentration again, leading to redissolution of the deposit formed. The corrosion phenomenon has thus a cyclic or pulsating nature, precipitation being followed by immediate redissolution. The balance between the flux of iron transported away from the surface and that injected due to corrosion is no longer an equilibrium between instantaneous stable fluxes, but between time-averaged values. The equilibrium which could not be attained by a pure direct formation mechanism is here obtained by restriction of the effective corrosion time. Indeed, transport in the solution occurs permanently, whereas metal dissolution takes place only during the fraction of time when the liquid has access to the metal, i.e. while the local iron concentration rises from the undersaturation threshold for redissolution to the supersaturation threshold for precipitation (Fig. 6b).

The transport equations derived for the pure mechanism remain valid, but on a time-averaged basis. In effect, there is no overall precipitation, and therefore no permanent flux of  $X^{n-}$  ions. There is simply a fluctuation in time of the local  $Fe^{2+}$  and  $X^{n-}$  concentrations, and the same  $X^{n-}$  ions shuttle back and forth between the liquid and the solid film on the metal. The essential features of a direct formation mechanism are indeed observed, but this time with  $Fe^{2+}$  cation control. This situation will therefore be described in abbreviated terms as an “insoluble cationic deposit”.

### 3.6. Corrosion beneath an insoluble cationic deposit

#### 3.6.1. Calculation of the corrosion rate

In both the intermittent and continuous regimes, the cumulated quantity of corroded iron remains equal to the cumulated quantity of  $H^+$  ions reaching the metal. Because the effective diffusion times are the same for both  $Fe^{2+}$  and  $H^+$ , the intermittence itself is not the major cause of regulation in the system, and the latter can therefore only arise due to the particular properties of the successive transient regimes.

These transients can be highly complex, particularly if the precipitation and redissolution are accompanied by the evolution or absorption of  $H^+$ . Nevertheless, even if only the diffusion transients are considered, it can immediately be seen that the latter are not symmetrical for  $Fe^{2+}$  and  $H^+$ .

In effect, iron only diffuses beyond the mean concentration  $Fe_s$  on the metal surface (Fig. 6c). However because by definition,  $Fe_s$  is less than the values  $Fe(d)$  corresponding to transport polarisation of  $H^+$  (Fig. 5a and b), the flux of iron is considerably reduced, and the same is therefore true for the flux of  $H^+$ .

In other terms, if the corrosion rate beneath a deposit becomes controlled by a transport polarization of  $Fe^{2+}$ , then the transport polarization of  $H^+$  can

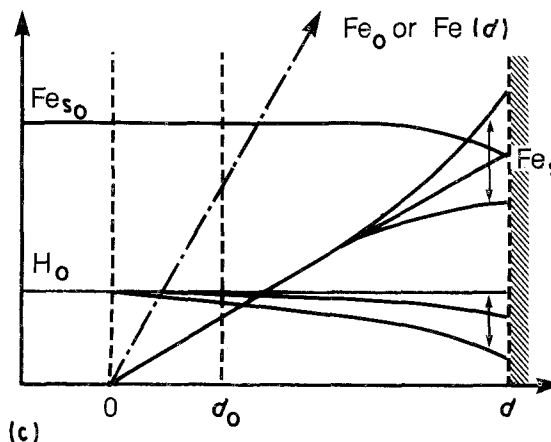
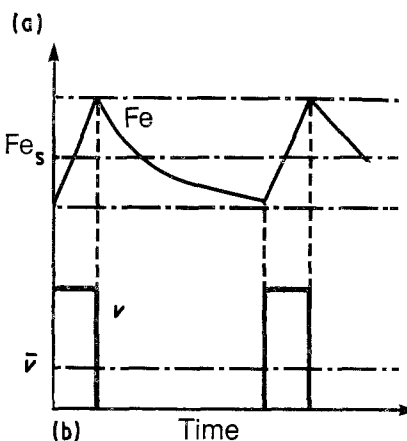
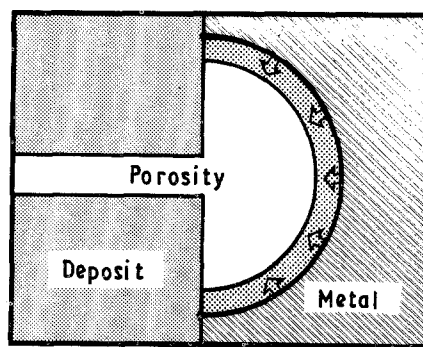


Figure 6 Corrosion beneath an “insoluble cationic” deposit. (a) Inhibition of corrosion by precipitation of solid products on the metal; (b) intermittent corrosion regime; (c) fluctuations in the  $Fe^{2+}$  and  $H^+$  concentration profiles.

only be very partial, or even negligible if  $Fe_0$  or  $Fe(d)$  is very much greater than  $Fe_s$ . Whereas  $Fe^{2+}$  continues to diffuse permanently, during a significant portion of the transients,  $H^+$  thus manages to get back to equiconcentration equilibrium, or to approach it quite closely. During these periods, the  $H^+$  flux becomes negligible again, so that the mean  $H^+$  flux decreases much more than that of iron.

In contrast to the pure direct formation mechanism, in this case, the reduction in the corrosion rate due to the deposit is a maximum when the potential corrosivity is controlled by an activation polarization.

In all cases, the corrosion rate beneath the deposit is given by

$$v = \frac{D}{K} \frac{\langle Fe(d) \rangle}{d} \approx \frac{D}{K} \frac{Fe_s(d)}{d} \quad (46)$$

where  $\langle \text{Fe}(d) \rangle$  is the time-averaged concentration of iron at the pore tip, theoretically close to the local iron solubility limit. Unfortunately,  $d$  cannot be calculated. It is the diffusion distance required for the difference between the  $\text{Fe}^{2+}$  and  $\text{H}^+$  transients to be able to balance their average fluxes.

### 3.6.2. Factors influencing the corrosion rate

In all cases, the formation of a corrosion deposit depends on local hydrodynamics, via the thickness  $d_0$  of the boundary diffusion layer, and also on the usual electrochemical parameters, via the potential corrosivity. However, the same is not necessarily true for the regulation of the deposit thickness, and therefore of the corrosion rate beneath the deposit.

For an insoluble cationic deposit, the corrosion rate is thus totally independent of the turbulence. In contrast, it remains sensitive to electrochemical effects, because the cathodic reduction of  $\text{H}^+$  is controlled at least partially by an activation polarization.

Finally, the only theoretical limitation to the existence of insoluble cationic deposits is that the redissolution of the scale at its outer surface must remain negligible compared to the redissolution of the newly created solid. This implies "ageing" of the deposit, with a change of allotropic form or of the zeta potential. Nevertheless, in  $\text{CO}_2$  [5] or  $\text{H}_2\text{S}$  [3] media, this is not particularly restrictive in view of the large variety of possible solids

## 3.7. Corrosion beneath an insoluble anionic deposit

### 3.7.1. Calculation of the corrosion rate

In an elementary diffusion model, according to Equation 45, depletion of the precipitable anion  $\text{X}^{n-}$  leads to an extremely simple  $\text{X}^{n-}$  concentration profile (Fig. 7):

$$X(x) = X_0 \left( 1 - \frac{x}{d} + \varepsilon \right) \quad (47)$$

The local solubility limit for iron is then given by Equations 10 and 47

$$\text{Fe}_s(x) = \text{Fe}_{s_0} \left[ 1 / \left( 1 - \frac{x}{d} + \varepsilon \right) \right] \quad (48)$$

Anionic control of the precipitation thus enables as much iron as necessary to be simply removed by diffusion. In contrast, it has no influence whatsoever on the liquid-phase transport of  $\text{Fe}^{2+}$  and  $\text{H}^+$ . The latter are therefore still controlled in the same way as in a pure direct formation mechanism, except that  $\varepsilon$  is as small as necessary for  $\text{Fe}_s(d)$  to attain the previously calculated  $\text{Fe}(d)$  level.

Because  $X_0$  is low, the anion flux  $J_X = D'X_0/d_0$  is itself small. The equilibrium between the  $\text{H}^+$  and  $\text{Fe}^{2+}$  fluxes is therefore displaced only very little. A very slight relative shift in the components of a mixed activation-diffusion polarization is then sufficient to introduce a deviation as small as  $J_X$  between the fluxes  $J_H$  and  $J_{\text{Fe}}$ .

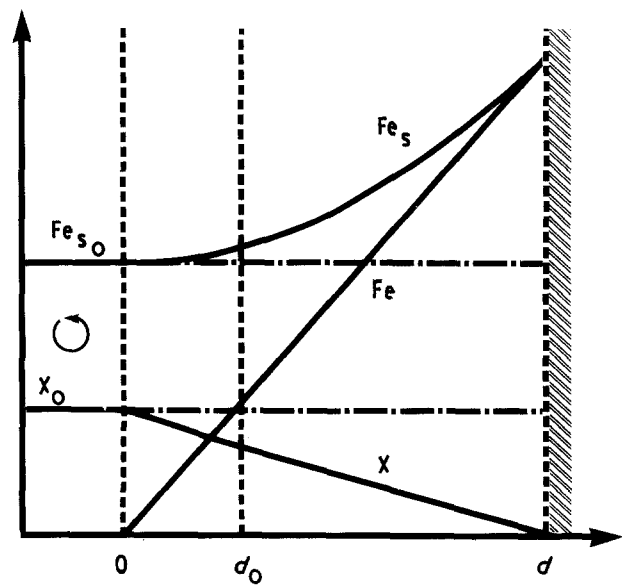


Figure 7 Corrosion beneath an "insoluble anionic" deposit:  $\text{Fe}^{2+}$  and  $\text{X}^{n-}$  concentration profiles, and spatial variation in the saturating iron concentration,  $\text{Fe}_s$ .

With regard to the corrosion rate, an insoluble anionic deposit is therefore equivalent to a pure direct formation mechanism where the precipitation beneath the scale is completely inhibited.

### 3.7.2. Factors influencing the corrosion rate

As for its cationic equivalent, the corrosion rate beneath an insoluble anionic deposit is sensitive to the electrochemical parameters and insensitive to hydrodynamic variables. On the contrary, because redissolution does not occur anywhere, an anionic deposit does not have the same theoretical limitation as its cationic counterpart. In particular, ageing of the deposit is not necessary, and it is sufficient for the dissolution kinetics to be low everywhere.

In fact, the most characteristic feature of insoluble anionic deposits is that they can be totally unprotective. Whatever the thickness, this happens if the potential corrosivity is controlled by activation polarization, and if, during growth of the deposit, "iron desaturation" occurs before the limitation of  $\text{H}^+$  transport. Such a situation is therefore encountered whenever  $X_0 \ll H_0$ . In contrast, if the potential corrosivity is already controlled by diffusion polarization, or if the limitation of  $\text{H}^+$  transport occurs before iron desaturation, an insoluble anionic deposit naturally has the protective effect corresponding to its thickness and to the resulting increase in diffusion polarization.

In practice, the unprotective insoluble anionic deposit model corresponds to the profuse scales observed at the bottom of the highly corrosive LACQ wells [9], or in wells of the same type in the Vienna basin [10, 11]. It even agrees particularly well with the apparently paradoxical explanations which had been proposed: precipitation of iron chloride under the sulphide [12], whereas  $\text{FeCl}_2$  is much more soluble than any of the iron sulphides; precipitation of  $\text{FeCO}_3$  beneath the sulphides, or of  $\text{FeS}$  in contact with the metal and  $\text{FeS}_2$  in contact with the external medium [10].

In fact, a stabilized insoluble anionic deposit, like any stabilized deposit, is not profuse. It can certainly be thick, but its thickness is stable. On the contrary, any non-stabilized scale which is profuse must necessarily be an insoluble anionic deposit. Indeed, it is the only type which can remain sufficiently unprotective not to become stabilized.

### 3.8. Corrosion beneath a soluble deposit

#### 3.8.1. Calculation of the corrosion rate

It is recalled that the notion of a soluble deposit is based on three prior conditions:

(i) precipitation of corrosion products occurs at a low supersaturation, the seeding effect favouring the formation of new solid on the rear face of the deposit (Fig. 8a);

(ii) precipitation is not limited by any transport phenomenon. Even if precipitation is heavy, corrosion and precipitation occur simultaneously and continuously at the metal surface;

(iii) in contrast, on the outer face of the deposit, steady-state redissolution occurs at the same rate as precipitation on the metal.

Because the precipitation occurs at a low iron supersaturation, it can be deduced that the kinetics of the precipitation and redissolution reactions are both rapid. In these conditions, the overall redissolution process must be controlled by the diffusion of the dissolved products [13]. The iron flux corresponding to this redissolution is therefore [13]

$$J_r = -D \frac{Fe_{s0}}{d_0} \quad (49)$$

If the pores are assumed to be fine, i.e. of diameter less than  $d_0$ , their presence in the dissolving surface in no way modifies Equation 49.

Moreover, the iron is at its local solubility limit at both ends of the pores, and as this limit varies little from one face to the other if anion transport is easy, the iron gradient and its flux  $J_1$  in the liquid phase remain small (Fig. 8b).  $J_1$  and  $J_x$  are then given by

$$J_x = -J_r = +D'' \frac{X(d) - X_0}{d} \quad (50)$$

$$J_1 = -D \frac{Fe_s(d) - Fe_{s0}}{d} \quad (51)$$

A limited expansion of the  $(Fe_s)^n X^2$  solubility product then yields

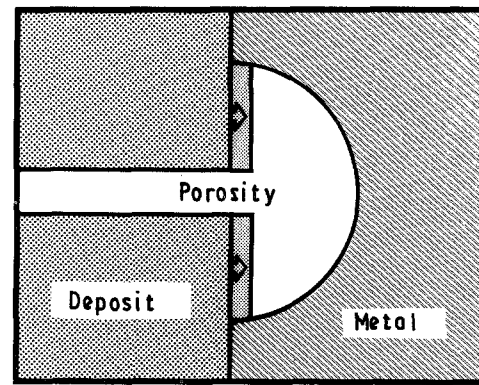
$$J_1 = + \frac{2D}{nD''} \frac{Fe_{s0}}{X_0} J_r \quad (52)$$

Furthermore, the material balance for the precipitation reaction can be written

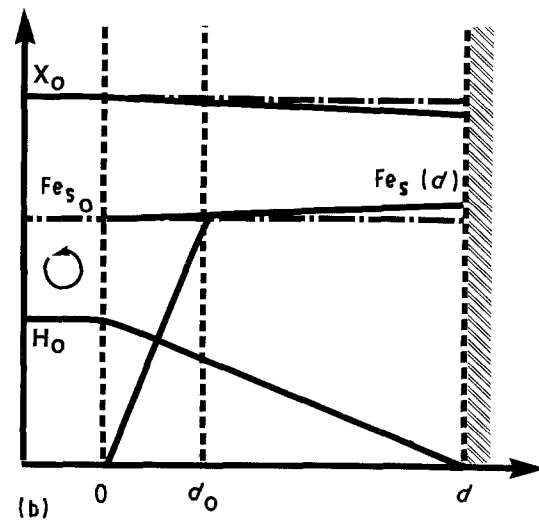
$$J_H + J_1 + J_r = 0 \quad (53)$$

where  $J_H$  is the  $H^+$  flux calculated for the pure direct formation mechanism (Fig. 5).

However, the sum  $J_1 + J_r$  is completely independent of the deposit thickness (Equation 52). During initial build-up of the deposit, the thickness therefore increases until it creates a transport polarization



(a)



(b)

Figure 8 Corrosion beneath a "soluble" deposit. (a) Precipitation on the rear face of the deposit; (b)  $Fe^{2+}$  and  $H^+$  concentration profiles, and spatial variation in the saturating iron concentration,  $Fe_s$ .

which limits the corrosion rate to the value permitted by redissolution (Equation 49), by the stoichiometry of the iron saturation in the corrosive medium ( $Fe_{s0}/X_0$ ), and by the relative mobility ( $D/D''$ ) of iron and of the precipitable anion.

#### 3.8.2. Factors influencing the corrosion rate

From the work of Levich [13], it could be suspected that the corrosion rate beneath a soluble deposit would depend on the local hydrodynamics. In fact, it will be seen that it depends *only* on the latter. While the thickness of the deposit is determined by the usual electrochemical parameters, it is totally compensated in this case by the diffusion barrier effect.

The soluble deposit thus appears to play a role in under-deposit corrosion equivalent to that of diffusion polarization in the case of corrosion of bare metal. A soluble deposit is therefore always protective.

## 4. Discussion

### 4.1. Summary of results

Although the diffusional models developed above are somewhat cumbersome (53 equations), they provide a considerable amount of information, which is summarized in Table I. While the effect of turbulence

TABLE I The influence of electrochemical and hydrodynamic parameters on deposit formation and on the corrosion rate beneath the deposit

Variable parameter (the others remaining constant)	Ease of deposit formation	Corrosion rate beneath the deposit		
		Insoluble cationic	Insoluble anionic	Soluble
Turbulence $\uparrow \nearrow$	$\downarrow \searrow$	=		$\uparrow \nearrow$
Potential corrosivity $\uparrow \nearrow$	$\uparrow \nearrow$	$\downarrow \searrow$	$\downarrow \searrow$	=
Proportion of diffusion polarization on the bare metal $\uparrow \nearrow$	=	$\uparrow \nearrow$	$\downarrow \nearrow$	=

seems quite intuitive, the influence of potential corrosivity is significantly less so, and the relative importance of activation and diffusion polarizations is not at all obvious.

The principal finding is even quite paradoxical, because all these models show that the protective character of a corrosion deposit is related neither to its composition nor to its morphology, but solely to its internal regulation mechanism (Fig. 3), i.e. to the structure of the corresponding diffusion model.

#### 4.2. General applicability of the results

Even if this is not always clear in the text, it has deliberately been chosen to treat the simplest situation, where: the oxidizing power of the medium is due only to  $H^+$ , and the precipitable anion  $X^{n-}$  cannot be hydrolysed and does not interact with  $H^+$ .

In a less simple case, such as corrosion by the acid gases  $CO_2$  and  $H_2S$ , it is also necessary to consider diffusion of the oxidizing molecules  $CO_2$ ,  $H_2CO_3$  and  $H_2S$ , and to take into account the two successive dissociations of carbonic acid and hydrogen sulphide, first to  $HCO_3^-$  and  $HS^-$ , then to  $CO_3^{2-}$  and  $S^{2-}$ . Similarly, for corrosion by oxygen, the diffusion of  $O_2$ , together with the water dissociation and oxide solubility equilibria, must also be considered.

Thus, while the results of the study cannot be directly transposed, the underlying principle remains generally applicable.

Moreover, it can be seen that a certain number of properties depend on the structure of the diffusion models rather than on particular parametral values. Models with the same structure will therefore automatically lead to a basic similarity in the properties of the corresponding systems. This is the case for example for corrosion by either  $CO_2$  or  $H_2S$ .

#### 4.3. Transitions from one type of deposit to another

The three diffusional models presented above were developed for the same chemical species, based on a single intrinsic hypothesis, i.e. the deviation from equilibrium required to initiate either precipitation or dissolution. The remainder is simply a matter of relative proportions in the composition of the corrosive medium.

It therefore ensues that continuous transitions can occur between the three models. Between a soluble

deposit and an insoluble anionic deposit, or between insoluble anionic and cationic deposits, the transition can be obtained indifferently by variations in either concentration, turbulence or electrochemical potential. The change from a soluble deposit to an insoluble cationic deposit, on the other hand, is not really a transition, in as far as it cannot be imposed voluntarily by continuous variations in potential or in the composition of the medium. On the contrary, if the effects are not clearly distinct, hybrid mechanisms may exist, with precipitation of new solid both on the deposit and on the metal, the corroded iron being transported in almost equal amounts in the liquid and solid phases. In contrast to genuine transitions, such hybrid situations remain perfectly fortuitous.

Overall, depending on the circumstances, in the case of uniform corrosion, the same salt can lead to three quite different types of deposit, in terms of their properties and protective nature.

#### 4.4. Stability of the uniform corrosion mode and the risk of localized corrosion

Each of the three types of deposit considered has a perfectly stable mode of regulation. Any given condition will therefore necessarily lead to a uniform mode of attack, with a single clearly defined corrosion rate.

On the contrary, if, on a portion of the surface, some external action artificially initiates a deposit which differs from the pre-existing type, then the couple so-formed introduces specific local conditions, which are different for each of the two deposits. Electrochemical polarization due to galvanic coupling can therefore stabilize, side-by-side, two deposits of different types and properties. Corrosion will then occur locally at two different rates, with all possible variations between general non-uniform corrosion and genuine local attack.

The case of localized attack by  $CO_2$  has already been extensively studied [14]. Nevertheless, the question still arises as to the precise nature of the coupling and the direction of progression of the rapid corrosion [2]. Similarly, cases of localized corrosion by  $H_2S$  have also been reported [9-12], with relatively unprotective profuse deposits on the anodes, and highly protective thin deposits on the cathodes. This confirms the basic similarity between  $CO_2$  and  $H_2S$  corrosion, the only difference being in the levels of solubility of the corresponding iron salts.



#### 4.5. The role of turbulence and the risks of erosion–corrosion

In the presence of irregular turbulence, the corrosion rate beneath a soluble deposit varies in the same manner as on the bare metal. Both the metal and the deposit will then be quite smooth, with the veins of liquid clearly outlined.

On the contrary, beneath an insoluble deposit, there will be no sign of the turbulence or of its irregularity, at least as long as the mechanical strength of the deposit has not been exceeded. However, if a fragment of the insoluble deposit is removed mechanically, then, because of the local galvanic couple, the one which reforms will not necessarily be of the same type. If this leads to local attack, then for a certain time at least, the latter will follow the contour corresponding to the critical shear stress necessary to break off the original deposit. This explains the origin of the well-known “horseshoe”, “heart-shaped” or “comet-tail” morphologies.

Furthermore, in both cases considered, the present study explains why the metal surface is not necessarily found to be bare in the zones affected by erosion–corrosion.

#### 4.6. The role of cations

In the models which have been developed, only a single possible solubility equilibrium has been considered, that of the  $\text{Fe}_n\text{X}_2$  salt. However, in the same way that the  $\text{X}^{n-}$  anion can interact with  $\text{H}^+$  in the case of a weak acid with a pH close to its pK value (cf. Section 4.2), it can also interact with cations other than iron, for instance with  $\text{Ca}^{2+}$ . Thus, in the case of  $\text{CO}_2$  corrosion in a formation water, the corrosive medium is generally already saturated or close to saturation in  $\text{CaCO}_3$  [14]. Local changes in acidity or in the degree of iron saturation then correspond to multiple buffers which need to be modelled in detail [5].

#### 4.7. The case of neutral media with local alkalinity

In the case where the cathodic reaction is the reduction of water or oxygen in a neutral medium, the change of oxidizing species will not be the only modification which must be taken into account. In effect, the corrosion reaction produces not only one, but two ions which take part in the solubility equilibria, i.e.  $\text{Fe}^{2+}$  and  $\text{OH}^-$ . Two, three or four equilibria may then be involved, such as  $\text{Fe}_n\text{X}_2$  and  $\text{Fe}(\text{OH})_2$ , and possibly  $\text{Ca}_n\text{X}_2$  and  $\text{Ca}(\text{OH})_2$ .

If all other conditions remain the same, the local solubility of iron, and thus the maximum possible corrosion rate, must therefore be higher in calcium chloride than in sodium chloride solutions, whence the well-known, but hitherto unexplained specific corrosivity of calcium salts.

It is thus clear that many practices in the field of corrosion are based on the results of studies on bare or passivable metals, i.e. on cases where potential and real corrosivity are indistinguishable. Indeed, on bare

metal, the potential corrosivity depends on only a small number of factors: pH, oxidizing power and temperature. In contrast, beneath a corrosion deposit, the real corrosivity also depends on the transition between activation and diffusion polarization, on the turbulence, on the buffering power, on the ionic strength and on the nature of the anions and cations present. With such a large number of parameters, precise modelling is essential in order to have any chance of distinguishing the really influential factors from those which it might be possible to neglect in any given case.

Moreover, the corrosion deposit may be controlled by a whole series of solubility equilibria, leading to a stratified structure of several solid compounds [12]. The present study then shows that this stratification is not the cause of the protective behaviour, but simply the consequence of the deposit regulation mechanism.

#### 4.8. Outcome of the gaseous hydrogen

Throughout the preceding treatment, it has been implicitly assumed that the molecular hydrogen formed remained in solution, and could be removed to the outside by diffusion, without ever reaching its solubility limit. This is effectively what happens whenever there is transport polarization (even partial) of  $\text{H}^+$ . In effect, the diffusion rates of the  $\text{H}_2$  molecule and of the  $\text{H}^+$  ion are probably fairly similar, but the solubility of  $\text{H}_2$  is higher than the usual  $\text{H}^+$  concentrations ( $\sim 1 \text{ mmol l}^{-1}$ ). Gaseous hydrogen evolution will therefore never occur for any soluble deposit.

On the contrary, beneath the two other types of deposit, in concentrated acid media, or due to the direct reduction of water, the local production of molecular hydrogen can be very copious, and its rate of removal can be insufficient. If the local chemical potential of  $\text{H}_2$ , i.e. its bubble pressure, reaches the total system pressure, gaseous hydrogen will be evolved within the deposit itself, and may or may not entrain the destruction of the solid layer. The first case corresponds to the vertical corrosion grooves which are well known in the sulphuric acid industry, whereas the second situation leads to corrosion product foams, such as the rust or alumina foams sometimes encountered on highly charged sacrificial anodes [15].

#### 4.9. The effect of a biofilm and sulphate-reducing bacteria

With liquid-phase diffusion transport, a biofilm is equivalent to a corrosion deposit for all species which do not take part in the local metabolism. In effect, the presence of this gel film increases the thickness of the layer which must be penetrated by diffusion. In contrast, the biofilm represents a perfectly transparent layer for the chemical species produced *in situ* by the metabolism.

By displacing the transport equilibria in this way, in certain cases, the biofilm can modify the corrosion potential of the underlying metal, sometimes even to a quite spectacular extent [16], while in other cases it may have no influence whatsoever. Moreover, in

a more or less well-aerated corrosive medium, the transport polarization of  $O_2$  can lead to an anaerobic zone of variable dimensions within the deposit itself, in which sulphate-reducing bacteria can develop. Local enrichment in molecular hydrogen can also promote the development of hydrogenase-containing strains. On the contrary, as long as hydrogen evolution does not prevent the water from having access to the metal, the consumption of this molecular hydrogen by the bacteria could in no case have any effect on the corrosion rate. Indeed, the reaction products have no direct influence on the kinetics of a reaction as completely irreversible as corrosion [17].

Finally, the release of acid metabolic waste and  $H_2S$  beneath the deposit, in contact with the metal, is totally different in nature from the addition of the same chemical species to the external corrosive medium. It thus appears quite illusory to try to distinguish the role of bacteria from that of the metabolites [18]. In effect, the undesirable nature of the  $H_2S$  differs depending on the place where it is generated, and indeed, when comparing corrosion by  $CO_2$  and  $H_2S$ , the latter is often presented as "protective".

In reality, the deleterious effect of sulphate-reducing bacteria is thus due to a combination of two conditions, the wrong substance being released in the wrong place.

## 5. Conclusions

By quantitatively modelling the material transport mechanisms involved, together with the reactions which take place, not only at the metal surface, but also in its immediate vicinity, the present study provides an explanation of the well-known multifarious behaviour of corrosion deposits. Even in a case as simple as uniform corrosion in an acid medium, with  $H^+$  as the only oxidizing agent, and with the possibility of precipitation on the metal limited to a single non-hydrolysable salt, it is shown that three basic types of deposit can occur:

(i) soluble deposits (precipitation-redissolution mechanism);

(ii) insoluble cationic deposits (direct formation mechanism, controlled by transport of the metal cation);

(iii) insoluble anionic deposits (direct formation mechanism, controlled by transport of the precipitable anion).

Although these three forms have strictly identical compositions, their conditions of formation, their protective properties and their sensitivities to external parameters are extremely different. In particular, insoluble anionic deposits can be completely unprotective, even for large thicknesses, and may never even become stabilized, leading to profuse growth. In fact, the protective character of a corrosion deposit is related neither to its chemical composition nor to its morphology, but rather to its internal regulation mechanism, and to the structure of the corresponding diffusion model.

The method of modelling employed appears to be quite general, and could be transposed to any type of corrosion. However, the possible configurations and the various working hypotheses are so numerous that a general discussion is really impossible. Separate models would need to be constructed case by case, for each type of corrosion, taking account of the fine details of the physical chemistry of the specific corrosive medium. The method thus appears to represent the theoretical tool which was missing for treating important problems, such as the reliable prediction of uniform corrosion rates of steels in the presence of  $CO_2$  and  $H_2S$  under pressure, or the high corrosivity of calcium salt solutions compared to those of sodium.

Finally, the method provides an explanation for certain apparently paradoxical experimental observations, such as the formation or absence of corrosion deposits during testing, the presence of deposits on surfaces affected by erosion-corrosion attack, or bacterial corrosion.

The possible fields of application of this technique include areas where it could have great economic repercussions, such as for monitoring internal corrosion by electrochemical methods, or the prediction of corrosion rates at locations inaccessible to any form of inspection. In such cases, the potential benefits can fully justify the use of the somewhat unwieldy procedure involved.

## References

1. Y. ADDA, J. DUPOUY, J. PHILIBERT and Y. QUERE, "Eléments de Métallurgie Physique", Vol. 6 (la Documentation Française, Paris, 1982) Ch. 45.
2. J. L. CROLET and M. BONIS, *SPE Prod. Eng.* **6** (1991) 449.
3. P. H. TEWARI, M. G. BAILEY and A. B. CAMBELL, *Corr. Sci.* **19** (1979) 573.
4. C. DE WAARD and D. MILLIAMS, *Corrosion* **31** (1975) 177.
5. J. L. CROLET and M. BONIS, in "NACE Annual Conference CORROSION '89", Paper 17, NACE, Houston (1989).
6. J. L. CROLET, *Techniques de l'Ingénieur*, Article M153, Paris.
7. Y. ADDA and J. PHILIBERT, "La diffusion dans les solides" (PUF, Paris, 1966).
8. "Handbook of Chemistry and Physics" (The Chemical Rubber Co.)
9. L. A. JEAN, *Erdoel Erdgas Z.* **89** (1973) 107.
10. H. ZITTER, *ibid.* **89** (1973) 101.
11. L. SPEEL, *Mater. Perform.* **15**(8) (1976) 46.
12. P. R. RHODES, *Electrochem. Soc. Extended Abst.* **76** (1976) 300.
13. V. G. LEVICH, "Physicochemical Hydrodynamics" (Prentice Hall, Englewood Cliff, N.J., 1962).
14. J. L. CROLET and M. BONIS, *Oil Gas Eur. Mag.* **10** (1984) 68.
15. J. L. CROLET, L. SERAPHIN and R. TRICOT, *Mét. Corr. Ind.* **52** (627) (1977) 396.
16. A. DESESTRET, *Matér. Techniques* **74** (1986) 317.
17. J. O. M. BOCKRIS and A. K. N. REDDY, "Modern Electrochemistry" (Plenum Press, New York).
18. S. DAUMAS, J. CROUSIER and J. P. CROUSIER, *Mét. Corr. Ind.* **64** (749) (1988) 1.

Received 1 March 1991  
and accepted 3 June 1992